EVALUATION OF THE MECHANICAL BEHAVIOR OF 3D PRINTED CELLULAR METAMATERIALS WITH SPECIAL GEOMETRIES

Rareş SAVA, Dragoş Alexandru APOSTOL, Dan Mihai CONSTANTINESCU

"Politehnica" University of Bucharest, Department of Strength of Materials, Bucharest, Romania
Corresponding author: Dan Mihai CONSTANTINESCU, E-mail: dan.constantinescu@upb.ro

Abstract. The behavior of triply periodic minimal surfaces (TPMS) structures like Gyroid, Schwarz P and Schwarz D created by using the Rhinoceros 6 software was studied through experimental mechanical compression testing. The topologies were printed using additive manufacturing and the DLP technique in cubic volumes, having dimensions of 25x25x25 mm. They had different unit cell arrangements ranging from one unit cell and going up to 8x8x8 unit cells. The overall weight of the samples was kept approximately constant as the increase of cells number would not affect the weight for each topology. Cubes were subjected to static compression testing and elastic constants were established by using the digital image correlation (DIC) method. Failure patterns have been studied by analyzing the cells' collapse in compression.

Key words: cellular metamaterials, TPMS, 3D printing, mechanical testing, Digital Image Correlation (DIC), failure.

1. INTRODUCTION

Minimal surfaces have a long history of over 200 years. While working on variational problems, Lagrange came up with the following question: "How does a surface bounded by a given contour look like, when it has smallest surface area?". It is stated in [1] that this was the start of the research on minimal surfaces. The interest of Lagrange [2] lied in the general variational problems where he analyzed the maximization and minimization of different properties. This proved to be a complicated problem to study, mainly because in following it, mathematicians found themselves without the necessary tools to solve the partial differential equation for the unknown minimal surface. The physicist Plateau [3], after carefully observing the behavior of soap films, derived the first mathematical conjectures about minimal surfaces.

By definition, triply periodic minimal surfaces (TPMS) have translational symmetries in three independent directions, and it is understood that these surfaces do not present self-intersections. There is an abundance of minimal surfaces that have self-intersections, but because they are trivial in nature, these surfaces present no interest for further study, from a mathematical point of view [4]. From bio-photonic structures to butterfly wing scales, TPMS are found in many natural systems [5]. On top of this, TPMS offer an array of interesting applications in many areas of science. On a closer investigation of their unique characteristics, deep mathematical challenges appear in trying to solve and understand them. This is why these minimal surfaces have been closely studied and described by mathematicians from different fields [1]. The first examples of triply periodic minimal surfaces were discovered by Schwarz in 1865, [6], followed by his student Neovius in 1883, [7]. They described five triply periodic minimal surfaces, namely, Schwarz P (primitive), Schwarz D (diamond), Schwarz H (hexagonal), Schwarz crossed layers of parallels, and Neovius. Then, the most famous Gyroid surface was described by Schoen in 1970, [8], along with another eleven newly discovered TPMS.

Recent advances in 3D printing and automated assembly have enabled such complicated material geometries to be fabricated at low cost. These mechanical metamaterials have properties that are a function of their mesoscale geometry as well as their constituents, 1, leading to combinations of properties that are unobtainable in solid materials; however, a material geometry which achieves the theoretical upper bounds for isotropic elasticity and strain energy storage, the Hashin-Shtrikman upper bounds 17, has yet to be identified. This limits the performance of all material systems and is defined by the highest performance possible for a two-phase system, which is achieved by the single-crystal diamond and void system. A material that achieves the three theoretical bounds simultaneously will reach the maximum possible mechanical properties, this being a serious limitation and at the same time a difficulty in designing mechanical metamaterials.

Only closed-cell materials, which are composed of sheets (that exploit material constraint in two directions) rather than slender beams, are potentially capable of achieving the Hashin-Shtrikman upper bounds on isotropic elastic stiffness. Periodic foams with ordered unit cells – the closed-cell analogue to lattice materials - can reach the Hashin-Shtrikman upper bounds for an isotropic material. The geometric complexity of ordered three-dimensional closed-cell materials has historically made their study and utilization impractical, from both an analytical, predictive standpoint, and a manufacturing one. However, modern analysis tools and manufacturing techniques now allow for their computational exploration and fabrication at declining cost.

A recent paper 18, focused on TPMS, which can separate the constituents of a two-phase composite into non-self-intersected and intertwined regions, and discusses about some TPMS composites generated by the structural topology method can approach the upper and lower Hashin-Shtrikman bounds. They continued the work from [19] and analyzed several geometries, where the FEM simulation approach is tedious as millions of elements are required for accurately capturing the irregular and curved shapes of TPMS cellular materials. The authors, [18], used an alternative homogenization method based on fast Fourier transform (FFT) to extract the effective moduli of cellular materials composed of four types of TPMS, namely: Schwarz D, Gyroid, Neovius and Schwarz P surfaces. Generally, topology optimization must be considered for a numerical FE analysis.

TPMS structures can produce tailored complex structures for various applications and serve as substitutes for polymeric foams. In [20], six different types of TPMS structures (Neovious, Gyroid, Schwarz P, Lidinoid, split P, and diamond) printed with the material Z-Ultra were examined under quasi-static compression in terms of their energy absorption capabilities, mechanical properties, and weights, which were compared with those of expanded polystyrene foam. It was found that the Neovious, diamond, and Lidinoid structures were most suitable for substituting expanded polystyrene foam, especially in safety helmets requiring high specific energy absorption capabilities.

Present work puts the bases of developing a methodology by which TPMS can be 3D printed, mecanically tested and analyzed as to better understand their behavior and failure under compression. Such a preliminary taken steps aim towards future applications as sandwich panels made with TPMS cores to be used for low velocity impact applications.

2. GENERATION OF TPMS

The software for generating the surfaces, Rhinoceros 6 [21], was used during the 80 days free trial period offered by the parent company Robert McNeel & Associates in connection with two plug-ins: Millipede and Wavebird [22]. The goal was to create an isosurface in such a way that any coordinates in the form [x, y, z] satisfy the known approximated function of the TPMS that the isosurfaces represent. In order to create the isosurface, the "Iso surface" tool from the Millipede plug-in was used. This tool generates a mesh with the user's input values. These values are the results from the "Evaluate" tool in Grasshopper. The variables [x, y, z] are defined by a range of numbers in the interval [$-\pi$, π]. This is done by using the "Range" tool with the domain set to [$-\pi$, π]. A number slider is used to increase or decrease the divisions of the interval.

To let the "Iso surface" tool work it is also required a "Box" which is a scaling feature for the mesh. The "Iso Value" is a function that allows for an offset from the original function to be created. Ideally the offset should be 0, in order to have a perfect representation of the function but when is set to 0 the "Iso surface" function does not create a mesh, so the slider will be set to the smallest possible value 0.001. By using this process, a complete mesh can now be generated. A toggle set to "True" is used for the "Merge Vertices" function so that the "Iso surface" tool merges all the vertices together. Now, the program generates a complete mesh that is the representation of the function introduced. The mesh is basically one cell of the triply periodic surface and in order to multiply it an "Array" is used with slider for the x, y, and z count. Because the resulting meshes are not joined together, the "Join meshes and Weld" function is used from the Wavebird plug-in. Now the program is able to create an accurate representation of any given function in the domain [$-\pi$, π] and the mesh can be multiplied in any direction. The resulting mesh is just an isosurface and impossible to be 3D printed, as was the goal set in the beginning. To solve this problem the "Mesh Thicken" function is called. A slider controls the "Distance" which is the wall thickness of the shape. Also, to control the "smoothness" of the final mesh, the "Laplacian Smoothing" and the "Loop Subdivision" functions are used. The scheme of the program used in [22] to generate various triply minimal geometries, with different cell configurations, and can be seen in Fig. 1.

Fig. 1 – Configuration of the complete program in Grasshopper.

Figure 2 shows the representative unit cells and 4×4×4 cells for the Gyroid, Schwarz D, Schwarz P and Neovius surfaces. From one unit cell to 2×2×2 unit cells, 4×4×4 unit cells, 6×6×6 unit cells and 8×8×8 unit cells were created, respectively. Cubes with an approximately 25 mm side and with different cell counts were generated and later printed.

(a)   (b)

(c)   (d)

Fig. 2 – Generated unit cells and 4×4×4 cells are shown, as an example, for: a) Gyroid; b) Schwarz D; c) Schwarz P; d) Neovius.

The increase in cell number is done by multiplication of the cells, while retaining the overall size of the cube as being about the same. One way of measuring the impact of the increase in cells number is to examine the change in volume. The effective volume of material for each geometry was calculated using the "Volume" function from Rhino and the results can be seen in Table 1. The Neovius type cell was not considered later for 3D printing.

Table 1

Volume [mm^3] of the created TPMS geometries with different unit cells

Unit cells	Gyroid	Schwarz D	Schwarz P
1x1x1	1724.6	1998.8	1508.9
4x4x4	1917.5	2379.1	1516.7
6x6x6	1942.1	2427.0	1517.5
8x8x8	1953.2	2452.9	1517.9

It can be observed that the volume is approximately the same for each topology. The only main difference is that Schwarz P has the lowest and practically the same volume even if we increase the number of cells, and Schwarz D the highest volume. The results obtained for the Schwarz D configuration will be presented at Discussion.

3. MATERIALS AND METHODS

3.1. 3D Printing method and material

We used an Anycubic Photon 3D printer, developed and produced by Anycubic. This is a Digital Light Processing 3D printer. Digital Light Processing, frequently referred to as DLP, is a 3D printing method that is based, at its core, on stereolithography. This technology, just like classical STL printers, creates a solid 3-dimensional shape by curing resin one layer at a time. The curing of resin is achieved by subjecting it to ultraviolet radiation, using localized photopolymerization. The radiation process takes place in a container that is filled with liquid resin, which is a mixture of monomers, oligomers and photo initiators. This printing method is capable of producing models that have a high degree of complexity with microscale architecture and submicrometer precision [23]. On top of this, due to the fact that the printing is done exclusively in a liquid environment, no supports are required for the printing of porous and hollow geometries. This makes DLP printing the ideal method for producing lattice metamaterials, pneumatically actuated soft robots, and various other special geometries that require the construction of trusses or cavities [23]. The software used for slicing the STL files is the Anycubic Photon Slicer, offered by the manufacturer with the printer. The resin used for printing the cubes was the Anycubic UV 405 nm 3D resin, with the technical parameters established as, [24]: viscosity (25°C) – 552 mPa·s; liquid density – 1.1 g/cm³; solid density – 1.184 g/cm³. shrinkage – 0.071; curing time – 6…10 s; tensile strength – 23.4 MPa; elongation at break – 0.142.

Printing parameters were considered as: layer thickness – 0.3 mm; normal expose time – 12 s; off time – 1 s; bottom expose time – 150 s; bottom layers – 10. For the bottom layers a greater exposure time is assigned as to ensure a proper fixture to the printing bed. Printing times varied from 2.5 hours to 3.5 hours, depending on the geometry of the cube. Although, the size of the printing bed allowed for up to six parts to be printed at once, this caused the prints to fail due to the high suction force between the model and the FEP film. This led to two major failure mechanism: 1) the layers would not adhere properly to the previous one and float in the resin until it would adhere randomly to the part; so, the layers would not adhere and the exposure time decreased drastically, thus resulteing a resin which was not cured sufficiently, as concluded after some time when it was observed that the failed models would change color, from white to yellow; 2) when trying to print multiple models at once the high value of the suction force let the layers adhere to the FEP film, and cure on it.

After trying different configurations and orientation of the models on the printing bed, it resulted that the best choice, which resulted in a successful print, with no imperfections and a high degree of accuracy, was to print one model at a time, oriented vertically.

3.2. Mechanical testing and material properties

The mechanical properties of the material in tension and compression were established by using the digital image correlation (DIC) method and the ARAMIS system manufactured by GOM Gmbh, with two cameras having a resolution of 2 Megapixels.

Testing was done with a Zwick/Roell Z010 static machine of 10 kN at 2 mm/min. The Zwick/Roell Z010 was connected to a force transducer and the data acquisition system HBM MGCplus AB22A produced by

Hottinger Brüel & Kjaer GmbH. The ARAMIS system was also connected to the HBM MGCplus system, and the calibration of the force transducer signal gave 2 kN/V. Thus, the force-displacement correlation between the testing machine and the ARAMIS system was obtained. For DIC a caliber of 35×28 mm was used to be able to measure the distances between facets. These facets had a dimension of 13 pixels and had a distance between them of 9 pixels.

In Fig. 3a are shown cubes printed from solid material of 10×10×10 mm, 15×15×15 mm, and 20x20x20 mm 3D printed and tested in compression; different dimensions of the cubes were tested as to observe possible size effects which were not at all significant in these cases. The dog bone specimens from Fig. 3b for traction, following the dimensions established in standard ASTM D638 – 14, for being tested in traction, with a length of 80 mm, 8 mm width in the middle part of the specimen, and 3.2 mm thickness; the chosen length was suitable for printing in order to avoid the warping of the sample at the edges, on the printing bed. Three tests for each configuration were performed and only a representative result will be shown. Same printing parameters as for printing the TPMS cubes were considered.

(a)   (b)

Fig. 3 – Printed specimens for traction and compression prepared for DIC testing: (a) compression; (b) traction.

Using the same setup, the 3D printed TPMS configurations were evaluated in compression. Because of the complex shapes and the uniquely particular curves of the 3D geometries the ARAMIS system could not be used, as errors in the calibration stage were obtained. As a result, all the data was plotted in the form of force-displacement diagrams. In all the experiments, the testing speed was kept as 2 mm/min.

The maximum force and the corresponding displacement of the geometry was determined. This will be considered as the beginning of the topology failure. In Figs. 4a and 4b are shown the Schwarz P cubes after complete failure. Evidently the 6×6×6 unit cells (Fig. 4b) cube behaved better, being more rigid.

(a)   (b)

(c)   (d)
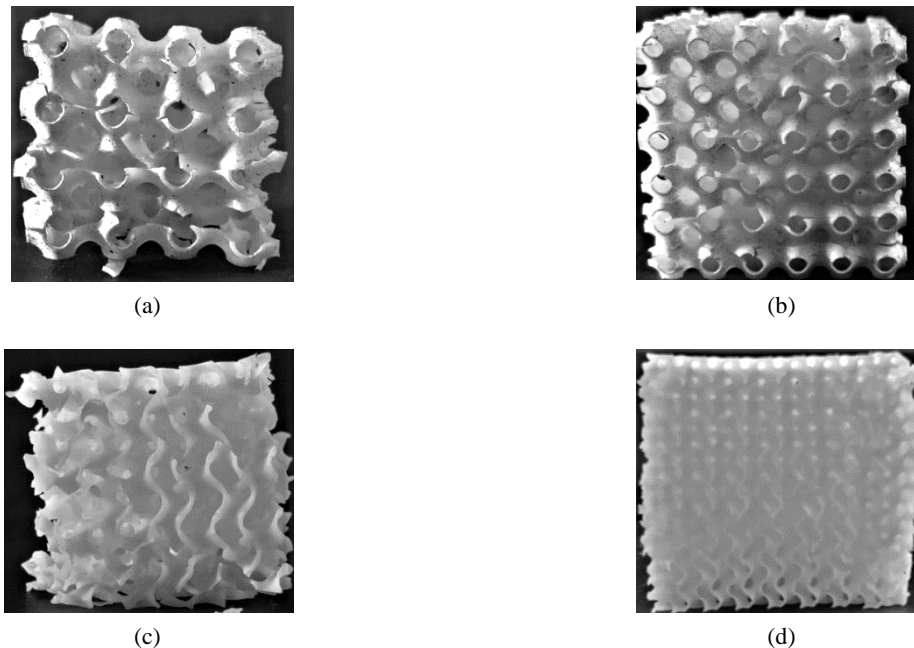
Fig. 4 – Printed cubes tested and failed in compression: a) Schwarz P 4×4×4 unit cells; b) Schwarz P 6×6×6 unit cells; c) Gyroid 6x6x6 unit cells; d) Gyroid 8×8×8 unit cells.

The Gyroid topology presented in Figs. 4c and 4d is even more sensitive to compression testing as the 6×6×6 cells cube was severely crushed. The 8×8×8 cell cube behaved much better, apparently not damaged, but in fact, during testing, the cells' walls were fractured successively, as it will be seen from the force-displacement diagram.

4. EXPERIMENTAL RESULTS

4.1. Material properties of the UV resin

Figure 5 depicts the relevant experimental results obtained for the UV resin. For compression testing (Fig. 5a) the Young's modulus was found to be in average about 1722 MPa, while nonlinear behavior appears at approximately 30 MPa. The specimens exhibit a barreling effect, which is typically met during a compression test. This effect is due to the friction of the sample with the compression plates. The determined results are within the range of similar materials found in literature and are comparable with the other types of UV sensible resins. For tensile tests (Fig. 5b), a typical DIC measurement revealed that strain at failure is about 8 % and the ultimate stress of the material is around 16.8 MPa. The Young's modulus had a value of about 1027 MPa. The Poisson's ratio was computed from DIC measurements by simulating a vertical and horizontal virtual strain gage and a value of 0.36 was determined.

So, the UV resin has a better behavior in compression, Young's modulus being 67 % greater than in tension, the material having a more fragile behavior. On the other hand, the tensile strength in tension is 16.8 MPa, a value which is smaller than 23.4 MPa, the one given by the producer.

(a)

(b)
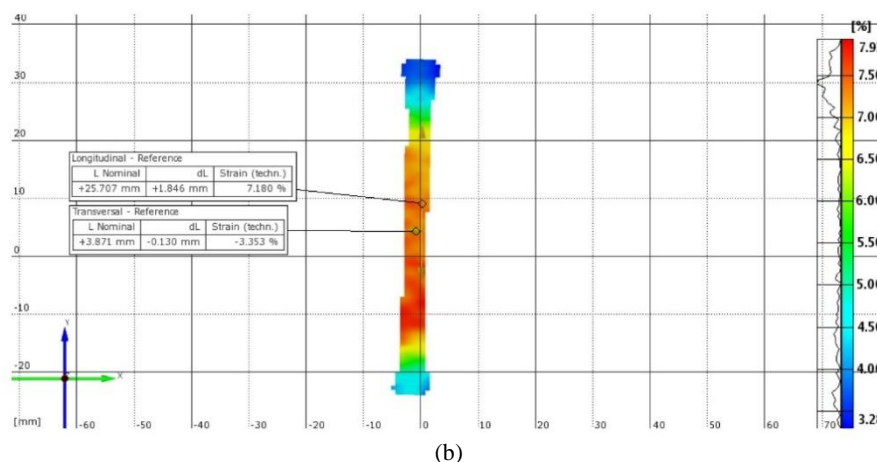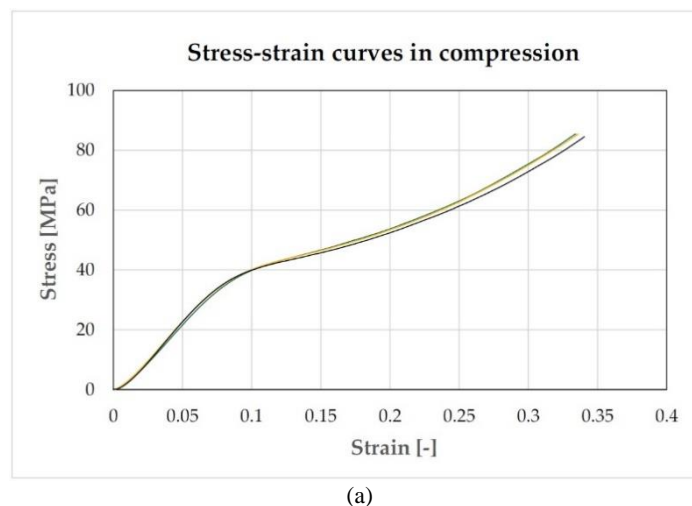
Fig. 5 – Experimental testing of UV resin: a) stress-strain curves obtained in compression;
b) traction test performed with ARAMIS.

4.2. Compression testing of TPMS cubes

For the printed cubic configurations, the obtained force-displacement curves in compression are presented in Figure 6 for all tests performed on the 8×8×8 unit cells for the Schwarz P (Fig. 6a) and Gyroid (Fig. 6b). Clearly, both TPMS exhibit successive cell wall failures as force is decreasing and increasing back. The Schwarz P cubes can sustain a force less than 400 N up to a global engineering strain of 50%. The Gyroid behaves much better, determining an average plateau force of about 800 N (specimen 3 behaved more poorly) until the displacement reached a value of 12 mm (coinciding with the densification process), when the load bearing capabilities of the structure were compromised.
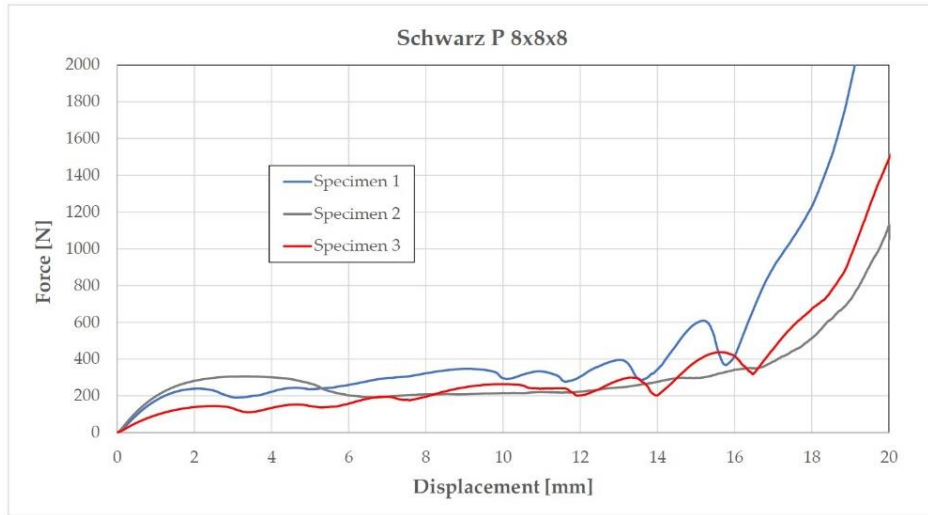
(a)
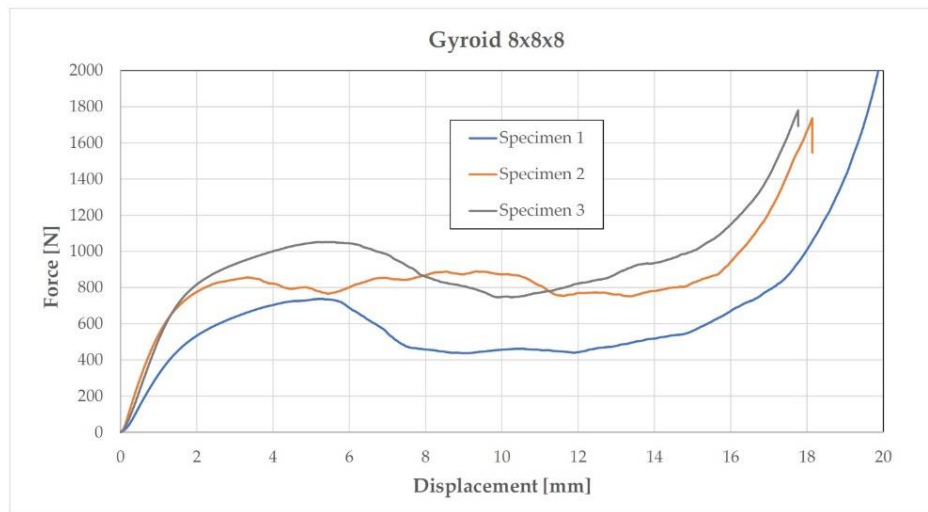
(b)

Fig. 6 – Response of 8×8×8 unit cells cubes in compression: a) Schwarz P; b) Gyroid.

From about 16 mm displacement in compression both topologies are severely crushed, and densification is evident. However, as seen also in Figure 4d, the Gyroid cube recovers surprisingly well, close to its initial dimensions.

When comparing the role of the number of unit cells in the compression response (Fig. 7), clearly for both Schwarz P and Gyroid the 1×1×1 and 2×2×2 configurations gave an extremely poor behavior. We have shown only one curve for each type of cells number as not to overcrowd the plots. For Schwarz P (Fig. 7a) we cannot clearly state that by increasing the number of unit cells we get an improvement in strength. For Gyroid (Fig. 7b) it is apparent that for the 8×8×8 unit cells configuration a much better response was obtained.
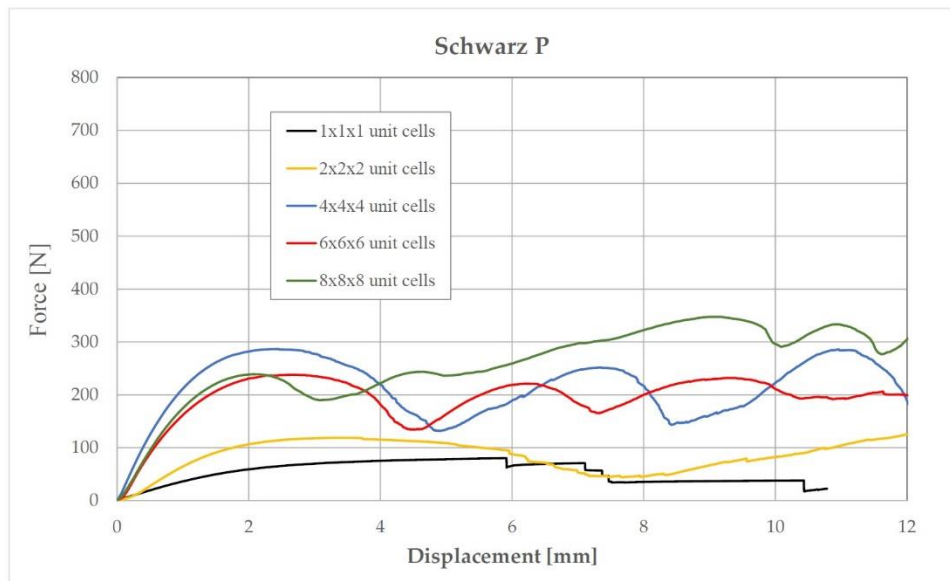
(a)
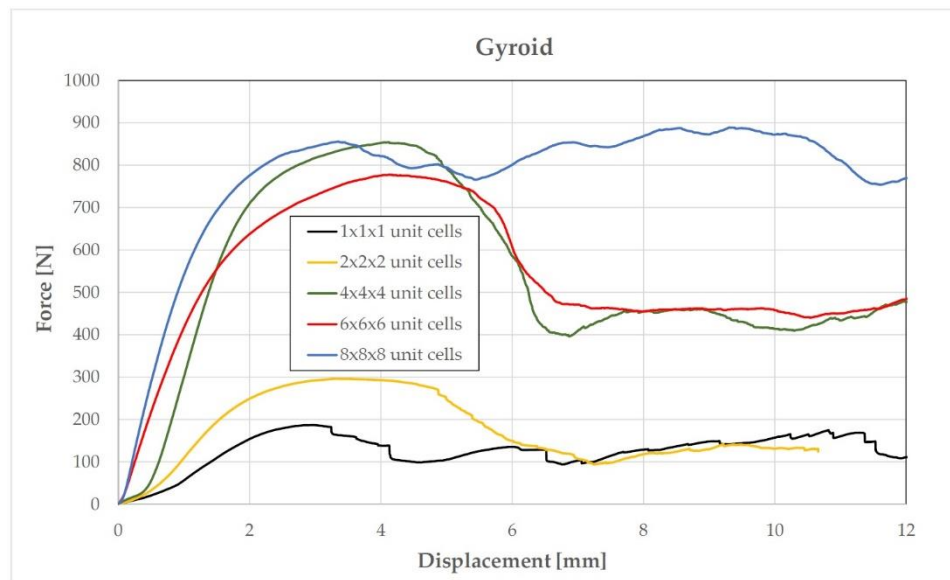
(b)

Fig. 7 – Influence of unit cells in the compression response of the cubes: a) Schwarz P; b) Gyroid.

4. DISCUSSION

The Schwarz D (Diamond) TPMS topology response in compression was not discussed up to now as the intricate geometry of such a structure leads to the necessity of testing in each direction, as the cube may exhibit different properties due to the anisotropic topology. As an example, in Fig. 8 are presented the resulted compression curves for the 8×8×8 unit cells configuration on the three orthogonal directions (1, 2 and 3 as in Fig. 8b) together with the same number of unit cells for Schwarz P and Gyroid structures. There is no clear assessment of the best positioning of the diamond cube with respect to the loading direction, as the variability of the obtained compression curves is high. However, this topology may be an alternative to the Gyroid.

Tests in compression for Schwarz D were done also for the other unit cells arrangements. As a general characteristic, failure occurred on a 45° plane. The failure mechanisms occur in the same manner regardless the unit cells number (Fig. 9). This topology is less reliable from mechanical point of view, being more susceptible to early collapse.

(a)   (b)
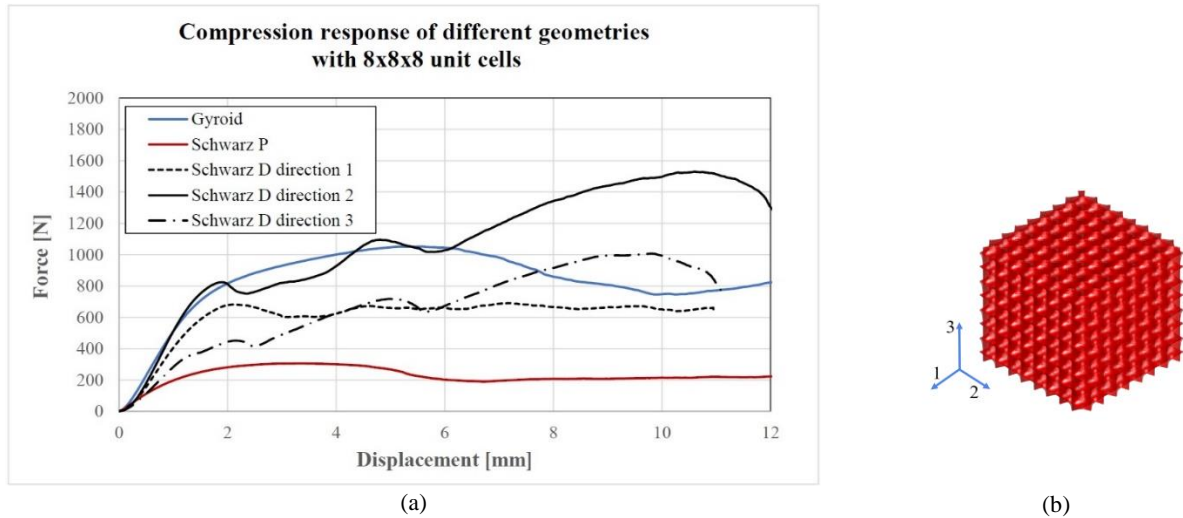
Fig. 8 – Different compression response for TPMS topologies: a) compression response for 8×8×8 unit cells for Gyroid, Schwarz D and Schwarz P; b) Schwarz D directions of testing notated as 1, 2, 3.

(a)   (b)   (c)
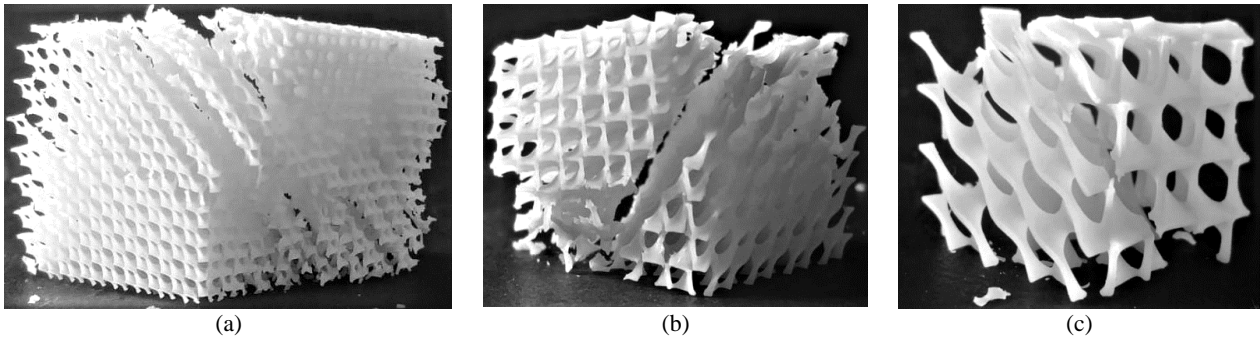
Fig. 9 – Failure of Schwarz D on 45° plane for: a) 8×8×8 direction 2; b) 6×6×6 direction 1; c) 4×4×4 direction 3.

So, a discussion on which of these topologies is better suited from the point of view of load bearing capability is needed further as being based on future testing. The Gyroid topology looks quite promising, especially when increasing the unit cells in the same volume. As mentioned in Table 1, using the "volume" function from Rhinoceros 6 software, for a volume of 1953 mm^3 and a density of 1.184 g/cm³ for the UV solid resin (as established by the producer), a mass of 2.31 grams results for 8×8×8 unit cells. In the plateau region the compression force is about 700–800 N. Compared to a closed cell polyurethane foam with a smaller density of 200 kg/m^3 (0.2 g/cm^3) tested in compression at room temperature for cubes of 12×12×12 mm, the stress in the plateau region is about 5 MPa [25]. That is, having a mass of 3.12 grams the resulting compression force is about 720 N. The Gyroid TPMS cube of 25×25×25 mm is lighter than the twice smaller polyurethane foam cube, having a mass smaller with 26 %.

6. CONCLUSIONS

The Gyroid topology proves to be very promising considering the strength mechanical response, also possessing an impressive recovering behavior, especially when the unit cells number is increased. For large volumes, the use of the Gyroid as an infill in different construction applications is a serious option. As mentioned in the previous chapter, this topology has, however, a better mechanical behavior when cell sizes are reduced, that is rigidity is increased. Still, for the moment, 3D printing of such topologies is expensive and time consuming. Overall, TPMS can be utilized in applications where optimal material usage versus porosity are required, such as heat exchangers and tissue engineered structures.

Schwarz D is a good strength competitor, but the intricate geometry favorizes significant shearing failure. The same geometry has single smooth surface and a huge potential for the fabrication of compact lightweight fuel cells with high energy density.

ACKNOWLEDGEMENTS

REFERENCES

1. H. KARCHER, K. POLTHIER, *Construction of triply periodic minimal surfaces*, Philos. T. R. Soc. A, **354**, pp. 2077–2104, 1996, https://doi.org/10.1098/rsta.1996.0093.
2. J.-L. LAGRANGE, *Matematica, Oeuvres de Lagrange*, Gauthier-Villars, Paris, 1867–1877.
3. J.A.F. PLATEAU, *Statique expérimentale et téoretique des liquides soumis aux seule forces moléculaires*, Gauthier-Villars, Paris, Trübner et Cie, Londre, 1873.
4. H. KARCHER, *The triply periodic minimal surfaces of Alan Schoen and their constant mean curvature companions*, Manusc. Math., **64**, pp. 291–357, 1989.
5. L. HAN, S. CHE, *An overview of materials with triply periodic minimal surfaces and related geometry: from biological structures to self-assembled systems*, Adv. Mater, **30**, art. 1705708, 2018, https://doi.org/10.1002/adma.201705708.
6. H.A. SCHWARZ, *Ueber die Minimalfläche, deren Begrenzung als ein von vier Kanten eines regulären Tetraeders gebildetes räumliches Vierseit gegeben ist*, Monatsberichte der Königlichen Akademie der Wissenschaften zu Berlin, pp. 149–153, 1865.
7. E.R. NEOVIUS, *Bestimmung Zweier Spezieller Periodischer Minimal flächen*, Akad. Abhandlungen, Helsinki, 1883.
8. A.H. SCHOEN, *Infinite periodic minimal surfaces without self intersections*, NASA Technical Report D-5541, USA, 1970.
9. M.F. ASHBY, *Hybrid materials to expand the boundaries of material–property space*, J. Am. Ceram. Soc., **94**, pp. s3–s14, 2011, https://doi.org/10.1111/j.1551-2916.2011.04559.x.
10. T. GEORGE, V.S. DESHPANDE, H.N.G. WADLEY, *Hybrid carbon fiber composite lattice truss structures*, Compos. A, **65**, pp. 135–147, 2014, https://doi.org/10.1016/j.compositesa.2014.06.011.
11. M.F. ASHBY, T. EVANS, N.A. FLECK, J.W. HUTCHINSON, H.N.G. WADLEY, L.J. GIBSON, *Metal foams: a design guide*, Butterworth-Heinemann, Boston, 2000.
12. D. JANG, F. MEZA, F. GREER, J.R. GREER, *Fabrication and deformation of three-dimensional hollow ceramic nanostructures,* Nat. Mater., **12**, pp. 893–898, 2013, https://doi.org/10.1038/nmat3738.
13. L. MONTEMAYOR, V. CHERNOW, J. R. GREER, *Materials by design: using architecture in material design to reach new property spaces*, MRS Bull., **40**, pp. 1122–1129, 2015, https://doi.org/10.1557/mrs.2015.263.
14. J.L. GRENESTEDT, *Effective elastic behavior of some models for 'perfect' cellular solids*, Int. J. Solids Struct., **36**, pp. 1471–1501, 1999, https://doi.org/10.1016/S0020-7683(98)00048-1.
15. L. VALDEVIT, A.J. JACOBSEN, J.R. GREER, W.B. CARTER, *Protocols for the optimal design of multi-functional cellular structures: from hypersonics to microarchitected materials*, J. Am. Ceram. Soc., **94**, pp. s15–s34, 2011, https://doi.org/10.1111/j.1551-2916.2011.04599.x.
16. C.M. SPADACCINI, *Mechanical metamaterials: Design, fabrication, and performance*, <u>in</u>: *Frontiers of Engineering: Reports on Leading-Edge Engineering from the 2015 Symposium*, National Academies Press, 2016, pp. 85–98, https://doi.org/10.17226/21825.
17. Z. HASHIN, S. SHTRIKMAN, *A variational approach to the theory of the elastic behaviour of multiphase materials*, J. Mech. Phys. Solids, **11**, pp. 127–140, 1963, https://doi.org/10.1016/0022-5096(63)90060-7.
18. Z. CHEN, Y. MINXIE, X. WU, Z. WANG, Q. LI, S. ZHOU, *On hybrid cellular materials based on triply periodic minimal surfaces with extreme mechanical properties*, Mater. Design, **183**, art . 108109, 2019, https://doi.org/10.1016/j.matdes.2019.108109.
19. J.B. BERGER, H.N.G. WADLEY, R.M. McMEEKING, *Mechanical metamaterials at the theoretical limit of isotropic elastic stiffness*, Nature, **543**, pp. 533-537, 2017, https://doi.org/10.1038/nature21075.
20. R. MIRALBES, D. RANZ, F.J. PASCUAL, D. ZOUZIAS, M. MAZA, *Characterization of additively manufactured triply periodic minimal surface structures under compressive loading*, Mech. Adv. Mater. Struct., **29**, *13*, pp. 1841–1855**,** 2022, https://doi.org/10.1080/15376494.2020.1842948.
21. R. McNEEL &. Associates, *Rhinoceros 6*, available: https://www.rhino3d.com, accessed on 15 March 2022.
22. R. SAVA, *Testing of 3D printed cellular materials with special geometries*, Bachelor of Engineering Thesis, University POLITEHNICA of Bucharest, Bucharest, 2020.
23. L. GREGURIĆ, *What is a DLP 3D printer? – simply explained | All3DP*, available online, accessed on 5 April 2022.
24. Anycubic, *UV 405nm 3D Resin*, available online: https://www.3dprintersbay.com/anycubic-resin, accessed on 15 March 2022.
25. D.M. CONSTANTINESCU, D.A. APOSTOL, *Performance and efficiency of polyurethane foams under the influence of temperature and strain rate variation*, J. Mater. Eng. Perfor., **29**, pp. 3016–3029, 2020, https://doi.org/10.1007/s11665-020-04860-4.